Numerical Behaviour of Blind-Bolted Beam Connections to Square Hollow Sections with Different Infills

Sahin Gunes[1] | Marios Theofanous[1] | Konstantinos Skalomenos[1] | Charalampos Baniotopoulos[1]

Correspondence

Dr. Konstantinos Skalomenos
Dept. of Civil Engineering
University of Birmingham
United Kingdom
B15 2TT
Email: k.skalomenos@bham.ac.uk

[1] University of Birmingham, Birmingham, United Kingdom

Abstract

This paper reports the development and validation of an advanced FE model that can predict the overall behaviour and failure modes of blind bolted T-stub to unfilled tube (UT), concrete-filled tube (CFT) and foam-filled tube (FFT) joints in tension. The joints investigated were made of S355 Square Hollow Sections (SHS) either empty or with concrete or polyurethane infill, connected to a rigid T-stub using HB 10 hollow bolts. Associated experimental results are used for model validation purposes. The main modelling assumptions and relevant simulation strategies in terms geometric and material modelling are discussed and the resulting models are shown to accurately replicate the experimentally observed response in terms of yield load, failure load, observed failure modes and available ductility of the connections. The favourable performance of connections employing SHS with a polyurethane infill compared to the empty and concrete filled SHS in terms of both strength and ductility is highlighted.

Keywords

Blind-bolted connections, Concrete-filled hollow section, Foam-filled hollow section, Numerical analysis

1 Introduction

Structural hollow sections (SHS) are becoming popular in the construction industry due to both their aesthetic appeal and favourable structural properties. They possess high stiffness about both major and minor axis thus making them very efficient against member buckling, have a high torsional stiffness and can also be filled with concrete [1,2] thus resulting in very strong and stiff members suitable for the very heavily loaded lower floor columns of multi-story buildings. Key to the successful application of either empty or concrete filled tubular members in construction is the existence of reliable and efficient design guidance, underpinned by relevant research.

Insufficient access due to the closed form of the hollow sections necessitates the use of blind bolts, many types of which are commercially available, including Hollobolt (Lindapter International, UK), molabolt (ABS, UK), Huck Bolt (Huck International, USA), Flowdrill (Flowdrill B.V., Holland), and Ajax Blind Bolt (Ajax Fasteners, Australia). The response of the Hollo-bolts in tension as well as the strength and stiffness of T-stubs employing Hollo-bolts was numerically investigated by Wang et al. [3], who proposed a rather complicated analytical predictive model. Elghazouli et al. [4] studied the behaviour connections with different configurations of Hollo-bolts and angle cleats under monotonic and cyclic loading, whilst Wang et al. [5] studied full-scale beam to tubular column joints employing hollow bolts and end plates. The ultimate behaviour of

blind-bolted beam to tubular column joints under high strain rate axial and shear loads was investigated by Liu et al. [6,7], whilst Elflah et al. [8] investigated experimentally and numerically the performance of stainless steel beam to tubular column joints.

Despite the existence of several types of blind bolts during the time that EN 1993-1-8 [9] was drafted, no design equations are provided for the stiffness and strength of the joint components/springs simulating the face of a tubular column in blind-bolted joint. Hence the design of blind bolted joints is based either on design recommendations made by researchers or manufacturers, which however do not have the status of codified design provisions. All available design recommendations for the strength of the column face in bending are based on yield line analysis of the face of the tubular column and involve analytical or numerical determination of the yield line pattern of the column face. Originally developed for the determination of the strength of blind-bolted connections executed with the flowdrill process, Yeomans [10] developed a design equation which was later adapted to blind-bolted connections using Hollo-bolts. This equation has been adopted by CIDECT in its design guidance on connections to hollow section columns [11]. A similar approach was developed by the SCI [12]. Gomes et al. [13] proposed a design model for the moment resistance of beam-to-open column joints with the column being bent about its minor axis. They identified two failure mechanisms, one related to failure of the column web in bending ("flexural mechanism")

and one related to punching shear ("punching shear mechanism") and proposed design equations for both. However, this design approach was shown to produce consistently unsafe results [5].

Further research aiming to improve the performance of blind-bolted joints led to the development of the Extended Hollobolt (EHB), specifically designed for concrete infilled columns [14-17], as the bolt extension provides an anchor in the concrete leading to the bolt developing its full tensile strength as opposed to the alternative where the blind bolt pulls out prematurely. Nevertheless, none of the previous studies have studied the performance blind bolted connections to hollow section columns with foam infill. Therefore, this study focuses on investigating the potential application of foam filled hollow section joint. Following the experimental study reported in [1], this paper reports a numerical analysis on blind bolted T-stub connections to empty, concrete filled, and foam filled SHS.

2   Development of FE model

The general purpose FE software ABAQUS [18] was used for the development of the nonlinear finite element models which were validated against the experimental test results reported in [1]. The measured geometry of the specimens was simulated, whilst the employed support conditions simulated the ones used in the tests. All joint components were discretised with the eight-noded 3D solid element C3D8R with reduced integration, except for the welds between the web and the flange of the loading T-stub, which were simulated using tie constraints. A finer mesh was employed in areas of high stress gradients like in the vicinity of the bolt holes, and throughout the blind bolt assemblies, whilst 3 elements were used through the thickness of each component to mitigate shear locking [8, 19, 20].

Given the complex geometry of the Hollo-bolt and the various interacting part it comprises, a pragmatic approach was followed, and the geometry of the various parts was simplified without compromising accuracy. The bolt shank was assumed to be prismatic, whilst a smooth geometry was assumed for the sleeve and the cone as well. A typical FE mesh of the various components constituting a model is depicted in Figure 1.

Hard contact was assumed in the normal direction, whilst the penalty method with a friction coefficient equal to 0.3 was used to simulate contact in the tangential direction [21], in accordance with the modelling assumptions reported in similar studies [7,18,19]. Finite sliding was assumed between all components in contact.

Classic Von-Mises plasticity with an elastic-isotropic hardening material response was assumed for the SHS and the experimentally obtained stress–strain curves for the steel used were converted into the true stress-logarithmic plastic strain format as required in [18]. The experimentally obtained yield stress was 406 MPa, whilst the ultimate tensile stress of the S355 steel was 509 MPa [1]. Due to the difficulty to carry out experimental tests on the sleeve of the hollo-bolts, their strength as stated by the manufacturer [22] was employed in the present study. Similarly, the M10 bolts were assumed to have a yield strength and

an ultimate tensile stress of 640MPa and 800 MPa respectively. Due to their large thickness compared to the stresses they were subjected to, the loading and reaction T-stubs were assumed infinitely elastic, which was verified by the absence of permanent deformation upon the completion of the tests.


Bolt shank shank   cone   sleeve   Anchored bolt

T-stub   hollow section   Anchored hollo-bolt

Concrete and foam   The view of anchored hollo-bolt
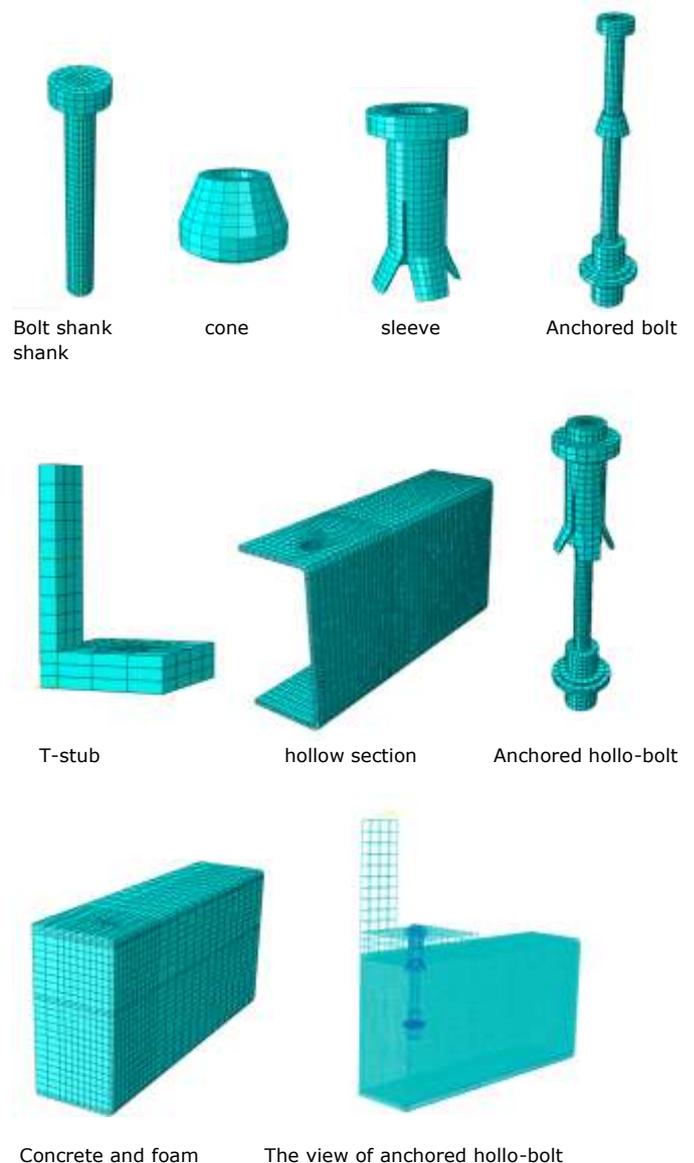
Figure 1 FE mesh of the various model components

The material response of the concrete infill was modelled using the concrete damage plasticity model available in ABAQUS [18]. Based on the average cube strength of 42.26 MPa reported in [1], all other material properties were determined following the approach employed in [23]. The values adopted for the relevant material parameters, namely the angle of dilation θ, the eccentricity, the ratio of equibiaxial to uniaxial compressive stress f_{b0}/f_{c0}, the ratio of the second stress invariant on the tensile meridian to that on the compressive meridian at initial yield K_c and the viscosity parameter were 40, 0.1, 1.16, 0.666 and 0 respectively. The chosen dilation angle of 40^0 was in between the range of 30^0 to 45^0 employed in similar studies [23], whilst the remaining values are the default values recommended in the Abaqus User Manual [18]. The tension stiffening of the concrete was modelled assuming a fracture energy $G_c=0.06$N/mm. This value is slightly larger

than the value of 0.055 N/mm corresponding to the recommendations of the Model Code for concrete with a maximum aggregate size of 8 mm.

Similarly, concrete damaged plasticity was employed to simulate the behaviour of the foam infill, which also displayed brittle failure under tension, however the experimentally obtained compressive stress-strain response [1] was utilised, whilst under tension a brittle fracture without tension stiffening was assumed. The material parameters for the concrete damaged plasticity model employed for the simulation of the foam were identical to those employed for the concrete with the exception of the uniaxial stress-strain curve under compression, which was adjusted according to the foam compressive strength. To avoid convergence issues brought about by incorporating the falling branch of material stress-strain response (i.e. concrete and foam), a quasi-static explicit dynamic analysis was carried out [23].

Since the specimens were symmetric with respect to two planes in terms of geometry, loading, support conditions and obtained response, to reduce computational time without compromising accuracy, a quarter of the model was simulated and suitable symmetry boundary conditions were applied along the planes of symmetry, as shown in Figure 2. The load was applied via displacement control of the top of the web of the loading T-stub.
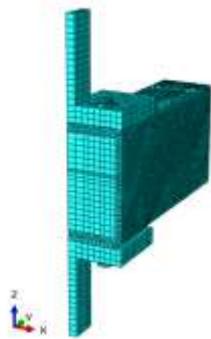

Figure 2 1/4 model of the simulated joint specimen

3   Results and Discussion

3.1   Failure modes

In Figure 3 the numerically obtained failure modes of the simulated connections are shown alongside the experimental ones [1]. Overall a good agreement between the numerical and experimental deformed shapes can be observed. The unfilled tube (UT) specimen exhibits significant flexural deformation of the column face in the vicinity of the bolt holes and partial pull-out of the blind bolts prior to sleeve fracture and subsequent pull-out of the bolt. The CFT specimen exhibits significantly reduced flexural deformations of the column face due to the concrete infill stiffening and strengthening the connection. Very limited bending deformations can be observed, and failure is caused by fracture of the bolt, thus proving the effectiveness of the concrete infill to prevent pull-out of the hollobolt. The FFT displays a failure mode similar to that of the UT, with failure caused ultimately by sleeve fracture and bolt pull-out upon failure of the structural foam infill. Foam

failure can be clearly observed in Figure 3 c), where a cone of the foam is clearly seen to fail.

a) Unfilled Tube

b) Concrete filled tube (CFT)

c) Foam filled tube (FFT)
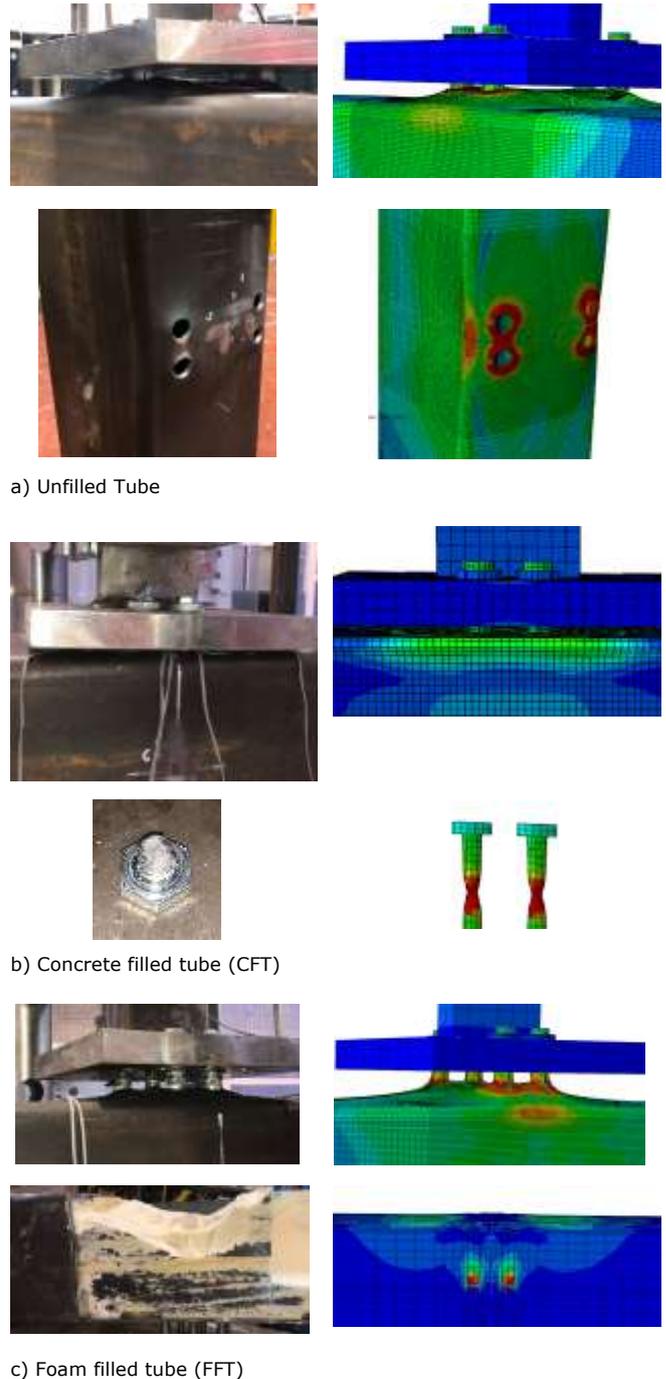
Figure 3 Experimental and numerical failure modes of the tested specimens.

3.2   Validation and Discussion

Following the comparison between the experimental and numerical failure modes, the numerically obtained load-displacement response is plotted together with the experimental one in Figure 4. Overall a very good agreement can be observed with the numerical curves closely following the experimental ones in terms of initial elastic stiffness, post-yielding stiffness, ultimate capacity, displacement at ultimate capacity and overall nonlinear response.
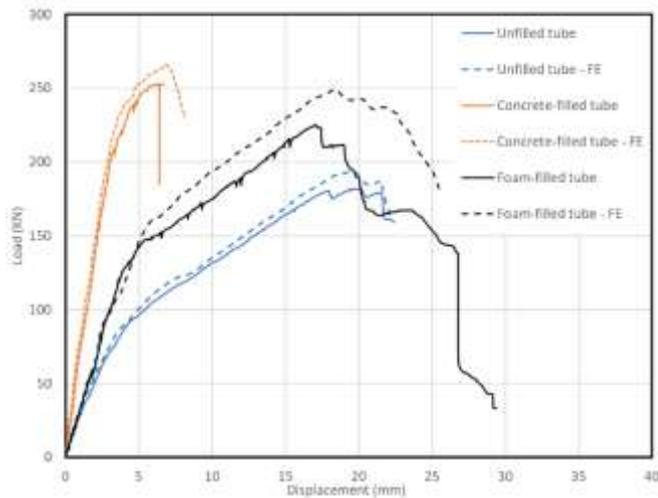
Figure 4 Experimental and numerical load-displacement response of tested specimens

To quantify the accuracy of the FE predictions with respect to the experimental tests, in Table 1 the ratio of the numerically predicted over the experimentally determined stiffness S_i, yield load F_y, ultimate load F_u and displacement at ultimate load δ_u is reported. In accordance with similar studies [25], the yield load was defined as the intersection between the initial elastic stiffness and the post-yield stiffness.

On average, the stiffness is well predicted however significant scatter between the predictions exists for the various specimens. This is not surprising given the sensitivity of the initial stiffness to the existence of gaps and slips between the various parts of the bolted connections that are hard to quantify and simulate [19]. The remaining three key quantities, namely the yield load, ultimate load and displacement at ultimate load are more consistently predicted but are slightly overestimated. In particular the predictions for the FFT seem to be the least accurate, which would indicate that further research is required to more accurately simulate the material behaviour of the foam infill.

Table 1 Accuracy of FE predictions for key behaviour quantities

| Speci-men | FE/Test | | | |
	Stiffness S_i	Yield load F_y	Ultimate load F_u	Displacement at ultimate load δ_u
UF	0.76	0.90	1.07	1.08
CFT	1.12	1.08	1.06	1.08
FFT	1.06	1.13	1.12	1.10
MEAN	0.98	1.04	1.08	1.08
COV	0.20	0.11	0.03	0.01

In terms of the observed response, it is noteworthy that a clear trade-off between strength and ductility seems to exist. As expected, the CFT connection exhibits the highest strength and stiffness owing to the effect of the concrete infill, which not only prevents the pull-out of the hollo-bolts but also disperses the bolt forces more evenly across the face of the SHS thus effectively eliminating the bending deformation of the column face. The low ductility associated with this specimen is due to the failure mode which essentially is bolt fracture. As clearly shown in figure 4, the deformation at failure is only twice the elastic deformation at yield whilst F_u/F_y ratio (ultimate over the yield load) is 1.20.

On the opposite end of the spectrum is the very ductile response of the UT connection. In the absence of infill, the overall response is significantly more flexible compared to the UT specimen with a clearly defined knee region corresponding to the plastic deformation of the column face in the vicinity of the bolt holes and an accompanying secondary stiffness due to inelastic response of the column face. The failure mode is shifted from bolt fracture to sleeve fracture, which occurs at a load 40% smaller to the one corresponding to the CFT connection. The ductility of the UT connection is significantly improved with a ratio of the displacement at ultimate over the displacement at yield being slightly over 4 and an overstrength ratio (F_u/F_y) equal to 1.90 (2.24 according to the FE results) thus indicating a very high inelastic reserve strength and very high ductility.

Finally, the novel FFT connection, which is intended to be a compromise between the strong but brittle CFT and the weak but ductile UT shows a response in-between the two extremes. Its ultimate load is just 11% lower than the CFT specimen and 24% higher than he UT one, with the corresponding F_u/F_y and δ_u/δ_y being equal to 1.66 and 3.7 respectively.

4   Conclusions

This study has reported the development of a nonlinear FE model that was shown to accurately predict the structural response of unfilled, concrete-filled and foam-filled SHS connected to a rigid T-stub via hollo-bolts, which simulates the tension zone of a moment-resisting beam to tubular column joint. The developed model can consistently predict the experimentally observed yield resistance and ultimate resistance with only a slight error, whilst the initial stiffness is less well-predicted. The analysis of the obtained results indicated the significant effect to of the infill (or absence thereof) of the strength, stiffness and ductility of the tension zone of the joints, which often controls the overall connection response. It was shown that for a modest loss of strength of 11% the ductility of the connection is significantly improved if the concrete infill is replaced by a more flexible foam one, which allows some limited plastic deformation of the column face prior to the ultimate failure of the connection, whilst still increasing the strength and stiffness of the connection significantly beyond that of an unfilled tube. Further research is underway to optimize the material characteristics of the foam infill to obtain tailored connection response to fulfil pre-determined strength and ductility requirements.

References

[1] Skalomenos K.; Gunes S.; Taleb, F.; Theofanous, M. (2023) *A comparative experimental study on blind-bolted beam connections to square steel tubular columns filled with polyurethane foam or concrete*. Proceedings of the 10th Eurosteel Conference on steel and composite structures, Amsterdam. Berlin: Ernst & Sohn.

[2] Skalomenos, K.A.; Hayashi, K.; Nishi, R.; Inamasu, H.; Nakashima, M. (2016) *Experimental behavior of concrete-filled steel tube columns using ultrahigh-strength steel*. Journal of Structural Engineering of ASCE 142, H. 9, 04016057

[3] Wang, Z.; Tizani, W. and Wang, Q. (2010) *Strength and initial stiffness of a blind-bolt connection based on the T-stub model*. *Engineering structures* 32, H. 9, p. 2505-2517.

[4] Liu, Y.; Malaga-Chuquitaype, C.; Elghazouli, A.Y. (2012) *Response and component characterisation of semi-rigid connections to tubular columns under axial loads*. Engineering Structures 41, p. 510-532.

[5] Wang, Z.-Y.; Wang, Q.-Y. (2016) *Yield and ultimate strengths determination of a blind bolted endplate connection to square hollow section column*. Engineering Structures 111, p. 345-369.

[6] Liu, Y.; Malaga-Chuquitaype, C.; Elghazouli, AY. (2012) *Response and component characterisation of semi-rigid connections to tubular columns under axial loads*. Engineering Structures 41, p. 510–532

[7] Liu, Y.; Malaga-Chuquitaype, C.; Elghazouli, A.Y. (2012) *Behaviour of beam to-tubular column angle connections under shear loads*. Engineering Structures 42, p. 434–56.

[8] Elflah, M.; Theofanous, M.; Dirar, S.; Yuan, H.X. (2019) Structural behaviour of stainless steel beam-to-tubular column joints. Engineering Structures, 184, p. 158–175.

[9] EN 1993-1-8 (2005). *Eurocode 3: Design of steel structures – Part 1-8: Design of joints*. CEN, Brussels.

[10] Yeomans, N. (1994) *I-beam/rectangular hollow section column connections using the Flowdrill system*. Proceedings Sixth International Symposium on Tubular Structures, Melbourne, Australia.

[11] Kurobane, Y.; Packer, J.A.; Wardenier, J.; Yeomans, N. (2004) *Design guide for structural hollow section column connections.* CIDECT. The international committee for research and technical support for Hollow Section Structures.

[12] SCI/BCSA (2005). *British constructional steelwork association joints in steel construction: moment connections*. Steel Construction Institute and the British Constructional Steelwork Association (P207).

[13] Gomes, F.; Jaspart, J-P.; Maquoi, R. (1996) *Moment capacity of beam-to-column minor-axis joints*. IABSE reports. p. 319–326.

[14] Pitrakkos, T.; Tizani, W. (2013) *Experimental behaviour of a novel anchored blind-bolt in tension*. Engineering Structures 49, 905–19.

[15] Pitrakkos, T.; Tizani, W. (2015) *A component method model for blind-bolts with headed anchors in tension*. Steel and Composite Structures18, 5, p. 1305–1330.

[16] Mahmood, M.; Tizani, W.; Sansour, C. (2015*) Effect of bolt gauge distance on the behaviour of anchored blind bolted connection to concrete filled tubular structures*. Proceedings of the 15th International Symposium on Tubular Structures. Rio de Janeiro. p. 87–93.

[17] Cabrera, M.; Tizani, W.; Ninic, J. (2021) *A review and analysis of testing and modeling practice of extended Hollo-Bolt blind bolt connections.* Journal of Constructional Steel Research 183, 106763.

[18] Hibbitt, H.; Karlsson, B.; Sorensen, P. (2011) *ABAQUS Analysis User's Manual Version 6.10*, Dassault Systèmes Simulia Corp.: Providence, RI, USA.

[19] Elflah, M.; Theofanous, M.; Dirar, S. (2019) *Behaviour of stainless steel beam-to-column joints—Part 2: Numerical modelling parametric study*. Journal of Construction Steel Research 152, p. 194–212.

[20] Yapici, O; Theofanous, M.; Yuan, H.; Dirar, S.; Afshan, S (2022) *Numerical simulation and design of ferritic stainless steel bolted T-stubs in tension*. Journal of Construction Steel Research 198, 107555.

[21] Skalomenos, K.A.; Hatzigeorgiou, G.D.; Beskos, D.E. (2014) *Parameter identification of three hysteretic models for the simulation of the response of CFT columns to cyclic loading*. Engineering Structures 61, p. 44–60.

[22] Lindapter International (2018). *Type HB Hollo-bolt for blind connection to structural steel and structural tubes*.

[23] Manos, G.C.; Theofanous, M.; Katakalos, K. (2014) Numerical simulation of the shear behaviour of reinforced concrete rectangular beam specimens with or without FRP-strip shear reinforcement. Adv Eng. Softw. 67, p. 47–56.

[24] CEB-FIP Model Code 1990 Bulletin d'information No.

196.

[25] Zanon, P.; Zandonini, R. (1988) *Experimental analysis of end plate connections*. Proceedings of the State of the Art Workshop on Connections and the Behaviour of Strength and Design of Steel Structures, Cachan. pp. 41–51.